International Journal of Engineering, Mathematical and Physical Sciences
ISSN: 2517-9934
Vol:7, No:4, 2013

Application of Novel Conserving Immersed Boundary Method to Moving Boundary Problem

S. N. Hosseini and S. M. H. Karimian

***Abstract*—**A new conserving approach in the context of Immersed Boundary Method (IBM) is presented to simulate one dimensional, incompressible flow in a moving boundary problem. The method employs control volume scheme to simulate the flow field. The concept of ghost node is used at the boundaries to conserve the mass and momentum equations. The Present methodimplements the conservation laws in all cells including boundary control volumes. Application of the method is studied in a test case with moving boundary. Comparison between the results of this new method and a sharp interface (Image Point Method) IBM algorithm shows a well distinguished improvement in both pressure and velocity fields of the present method. Fluctuations in pressure field are fully resolved in this proposed method. This approach expands the IBM capability to simulate flow field for variety of problems by implementing conservation laws in a fully Cartesian grid compared to other conserving methods.

***Keywords*—**Immersed Boundary Method, conservation of mass and momentum laws, moving boundary, boundary condition.

I. Introduction

THE Immersed Boundary Method (IBM) is a powerful approach for simulating flows in moving boundary and complex geometry problems. In this method discretization of equations are carried out on a Cartesian grid which is simple to generate. However the boundary does not conform to the grid lines and therefore indirect methods are employed to apply the boundary conditions. This creates a range of different methods developed in the context of IBM which are applied to elastic [1]-[5] and solid [6]-[9] boundaries. The methods generally employed so far for solid boundaries, use nodes (i.e. ghost nodes) in the Cartesian grid located outside the fluid to apply boundary conditions. The value of ghost nodes is set so as to meet the boundary conditions. In these methods, Finite Difference scheme is usually used to simulate the flow field and the ghost node value is determined using a kind of interpolation schemes [10]-[12]. Although these approaches are almost fast and simple, conservation of mass and momentum equations in boundary cells are neglected. There is also a different category of methods based on Cartesian grids called "cut cell" [3], [13]-[18] that implement conservation laws in boundary cells.

However the shape of Cartesian cells in the vicinity of boundary is changed to fit the boundary. In these methods cells are cut by the boundary which passes through them, and conservation laws are implemented in these cut cells conforming to the boundary. This approach is more complicated especially compared to IBM as the boundary may cut the Cartesian grids anywhere on the cells and create new boundary cell geometry. These cells are no longer a rectangular cell and are considered conformed to the boundary the way they are. This complicates the discretizing of equations and calculation of fluxes particularly in two and three dimensional and moving problems.

In the current study a control volume scheme based on IBM is proposed in which Cartesian grid is used even in the vicinity of the boundary. In this method the mass and momentum equations are conserved taking advantage of ghost nodes concept in IBM.

S. N. Hosseini is with Amirkabir Univeristy of Technology, Hafez Ave, Tehran, Iran (email: nhosseini@aut.ac.ir).
S. M. H. Karimian is with Amirkabir University of Technology, Hafez Ave., Tehran, Iran (email: hkarim@aut.ac.ir).

II. Numerical Algorithm

In this section, governing equations are described, and different control volume and node types encountered in present method are explained. This is followed by discretization of equations and implementation of boundary conditions. A detailed discussion of the method used for imposing the boundary condition is presented.

A. Governing Equations

Governing equations of one dimensional incompressible inviscid flow in a moving boundary problem for a control volume shown in Fig. 1 include the mass conservation equation of

$$\int_{cv_i} \frac{\partial \rho}{\partial t} dV + \int_{cv_i} \frac{\partial \rho (u - u_c)}{\partial x} dV = 0 \qquad (1)$$

and the momentum conservation equation of

$$\int_{cv_i} \frac{\partial \rho u}{\partial t} dV + \int_{cv_i} (\rho \frac{\partial \rho u (u - u_c)}{\partial x} + \frac{\partial P}{\partial x}) dV = \qquad 0(2)$$

Where u is the flow velocity in the x direction, ρ is density, P is pressure, u_c is the grid velocity and t represents time.

B. Control Volume and Node Types

The dotted area in Fig. 1 represents the Control volume of node i. Each Control Volume is surrounded by two integral points which are located halfway between two neighboring nodes and are depicted via cross symbol in Fig. 1.Three kinds of control volumes are presented in this method. The first control volume is the one that is in the middle of the solution

domain and does not contain the boundary as shown in Fig. 1. This control volume is called ordinary control volume. The node pertaining to this control volume is also an ordinary node.

The second control volume is related to a node which the boundary has passed from it but has not yet left its control volume. This control volume is called ghost control volume type one and is shown in Fig. 2. The node pertaining to this control volume is named a ghost node. The third control volume is related to a node which boundary has passed from it and has left its control volume.

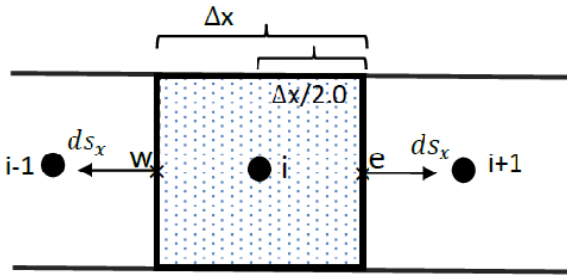

Fig. 1 Ordinary Control Volume

But since the boundary is still between this node, i.e. node i, and its neighbor node, i.e. node i+1, this control volume is called ghost control volume and is tagged as ghost control volume type two, in Fig. 3. In general whenever immersed boundary is located between two nodes, the node that is outside of the flow filed is called ghost node and its corresponding control volume is called ghost control volume. Immersed boundary is always treated by ghost control volumes. Note that in both cases control volume i+1 will be treated as an ordinary control volume; this will be described later.

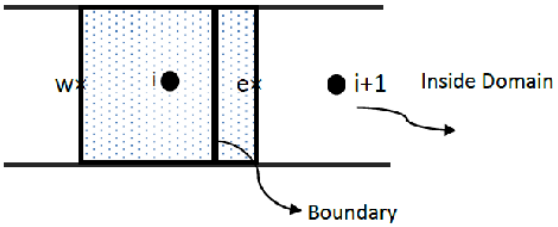

Fig. 2 Ghost Control Volume type one

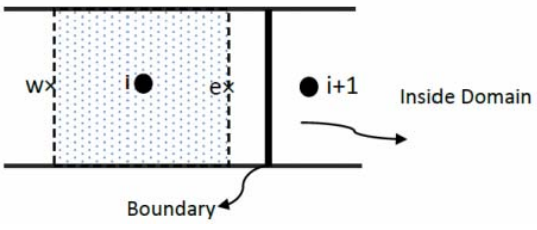

Fig. 3 Ghost Control Volume Type two

C. Ordinary Control Volume

In this part discretization of mass and momentum equations are carried out for ordinary control volume. Having substituted the volume integral in the second term of (2) with surface integral one can get:

$$\int_{cv_i} \frac{\partial \rho}{\partial t} dV + \int_{s_i} \rho(\hat{u} - \hat{u}_c) dA = 0 \tag{3}$$

Density is constant and in an ordinary control volume there is no change in volume. Therefore only the second term remains to be discretized between integral point's e and w as given below

$$\rho(\hat{u} - \hat{u}_c) ds_x|_e - \rho(\hat{u} - \hat{u}_c) ds_x|_w = 0 \tag{4}$$

In (4), $\hat{u}_c$ is the grid velocity which is zero since in contrast to the ordinary moving mesh methods [19], in IBM the grid is stationary and does not move. Mass conserving velocities $\hat{u}$ at integration points e and w are modelled as described in [20]. At integration point e this is given by

$$\hat{u}_e = \frac{u_i + u_{i+1}}{2} - \frac{1}{2\hat{u}_e}(P_{i+1} - P_i) \tag{5}$$

A similar equation is used to model $\hat{u}$at integration point w. Substitution of these definitions of $\hat{u}$ at integration points e and w in (5)

$$\begin{aligned} \rho\left\{\frac{u_i + u_{i+1}}{2} - \frac{1}{2\hat{u}_e}(P_{i+1} - P_i)\right\} ds_x \\ - \rho\left\{\frac{u_{i-1} + u_i}{2}\right. \\ \left. - \frac{1}{2\hat{u}_w}(P_i - P_{i-1})\right\} ds_x = 0 \end{aligned} \tag{6}$$

In which ds_xhas been assumed to be constant. Having applied a similar procedure used for the mass conservation equation, to the momentum conservation equation, (2), one can get

$$\begin{aligned} \rho \frac{u_i^{new} - u_i^{old}}{\Delta t} V_{cv_i} + \rho u(\hat{u} - \hat{u}_c) ds_x|_e + P ds_x|_e \\ + \rho u(\hat{u} - \hat{u}_c) ds_x|_w + P ds_x|_w \\ = 0 \end{aligned} \tag{7}$$

As mentioned previously, for an ordinary control volume $\hat{u}_c$is zero. Mass conserving velocities $\hat{u}_w$ and $\hat{u}_e$are calculated using their values from the previous linearization iteration. Convected velocities, u, at integration points e and w areupwinded and set equal to $u_i$and u_{i-1}respectively. Pressures at the integration points are averaged from their neighbor nodes. With these approximations (7) will become as

$$\rho\frac{u_i^{new}-u_i^{old}}{\Delta t}V_{cv_i}+\rho u_i\hat{u}_e ds_x|_e+\rho u_{i-1}\hat{u}_w ds_x|_w+\frac{P_{i+}P_{i+1}}{2}ds_x|_e+\frac{P_{i-1+}P_i}{2}ds_x|_e=0 \quad (8)$$

$ds_x|_e$ is considered unity and positive while $ds_x|_w$ is also unity but negative. V_{cv_i} is Δx as said before. Applying this to (8) we will have:

$$\rho\frac{u_i^{new}-u_i^{old}}{\Delta t}\Delta x+\rho\hat{u}_e u_i-\rho\hat{u}_w u_{i-1}+\frac{P_{i+1}}{2}-\frac{P_{i-1}}{2}=0 \quad (9)$$

Where ds_x has been assumed to be constant. Coefficients of velocity and pressure for each node are calculated after discretization of conservation of mass and momentum equations.

III. Applying Boundary Condition

The key point of the algorithm described in this paper is the discretization of conservation equations at the boundaries, i.e. for ghost control volumes that is described earlier

A. Ghost Control Volume Type One

As seen in Fig. 4, ghost control volume i that is known as type one includes an immersed moving boundary which has not left this control volume [21]. A part of flow field indicated by dots, is still in this ghost control volume. This dotted area is designated as the volume of ghost control volume i. We first write mass conservation equation for ghost control volume i, i.e. the dotted area. As seen in Fig. 4, a moving boundary causes volume change and this should be considered in the first term of the mass conservation equation, (1). Second term of (1) is evaluated between integral point e and boundary b. Therefore mass conservation equation for ghost control volume type oneis written as

$$\rho\frac{V_{new}-V_{old}}{\Delta t}+\rho(\hat{u}-\hat{u}_c)ds_x|_b^e=0 \quad (10)$$

or

$$\rho\frac{A.(x_e-x_{new})-A.(x_e-x_{old})}{\Delta t}+\rho(\hat{u}_e-\hat{u}_{ce})A-\rho(\hat{u}_b-\hat{u}_{cb})A=0 \quad (11)$$

Grid velocity at the integral point e is zero, i.e. $\hat{u}_{ce}=0$, and also $\hat{u}_b=\hat{u}_{cb}$. Therefore for a constant area duct one can get

$$\frac{x_{old}-x_{new}}{\Delta t}+\hat{u}_e=0 \quad (12)$$

Having calculated the first term geometrically and substituted $\hat{u}_e$ from (5) in (12), mass conservation equation for ghost control volume type one is obtained as

$$\frac{x_{new\_}x_{old}}{\Delta t}+\frac{u_i+u_{i+1}}{2}-\frac{1}{2\hat{u}_e}(P_{i+1}-P_i)=0 \quad (13)$$

The same procedure followed for the mass conservation equation is applied to (3) to obtain the following discretized form of momentum conservation equation for the ghost control volume type one.

$$\rho\frac{u_i^{new}V_{new\_}u_i^{old}V_{old}}{\Delta t}+\rho(\hat{u}_j-\hat{u}_{cj})u_i ds_x|_w+\rho(\hat{u}_j-\hat{u}_{cj})u_i ds_x|_b+P_w-P_b=0 \quad (14)$$

Substituting $u_{cw}=0$ and $u_b=u_{cb}$ in above equation it returns to:

$$\rho\frac{u_i^{new}V_{new\_}u_i^{old}V_{old}}{\Delta t}+\rho\hat{u}_w u_i+P_w-P_b=0 \quad (15)$$

Discretization of mass and momentum conservation equations for ghost control volume type one is closed. In the next section discretization of conservation equations for the ghost control volume type two is addressed.

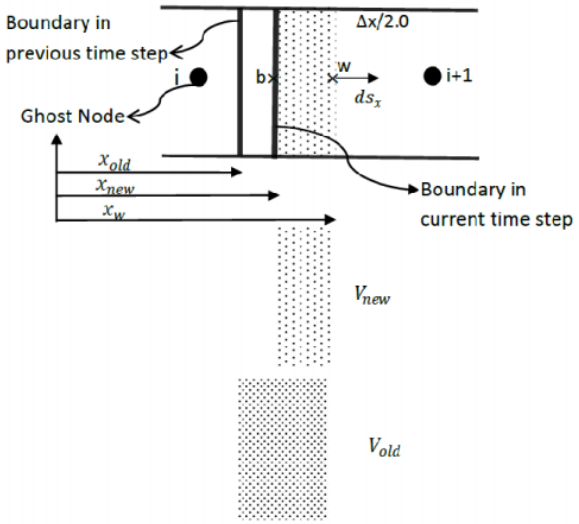

Fig. 4 Ghost Control Volume Type One

B. Ghost Control Volume Type Two

Consider ghost control volume iin Fig. 5, which is known as ghost control volume type two. This is a control volume that the boundary has left it but is still between its node, i, and its neighbour node, i+1, which is within the flow field. The control volume that should be considered here is the one between the boundary b and integral point e, shown by dotted area in Fig. 5. However we would like to remain in the general

frame work of IBM, i.e. consider control volume of every node within the flow field as a complete one and do not cut it to pieces. Therefore control volume of node i+1 is treated as an ordinary control volume between integral points w and e, illustrated by horizontal lines in Fig. 5. Boundary conditions, then will be treated throughout the ghost nodes. Based on this strategy nodes within the flow field are always considered as ordinary nodes and their corresponding control volumes are treated as complete control volumes. What so ever happens on the boundary is then treated by ghost control volumes. To handle this, the difference between the real control volume and the complete one, i.e. the volume between integral point w and boundary b, is assigned to the ghost control volume i as the subtracted volume, shown as dashed diagonal lines in Fig. 5.

At the boundary, conservation equations are written for the ghost control volume only. However these equations together with the conservation equations of control volume i+1will result in conservation equations for the real control volume, i.e. the dotted area. Here it is shown that how this strategy works.

Mass conservation equation, (3), for the ghost control volume i, i.e. the volume with dashed diagonal lines in Fig. 5, is given bellow.

$$\rho\frac{(V_{old}-V_{new})-0}{\Delta t}+\rho(\hat{u}_w-\hat{u}_{cw})ds_x|_w + \rho(\hat{u}_b-\hat{u}_{cb})ds_x|_b=0 \quad (16)$$

In which the volume at the present time step is $V_{old}-V_{new}$, and the volume at the previous time step is zero. For the control volume of node i+1, mass conservation equation can easily written as

$$\rho(\hat{u}_e-\hat{u}_{ce})ds_x|_e+\rho(\hat{u}_w-\hat{u}_{cw})ds_x|_w=0 \quad (17)$$

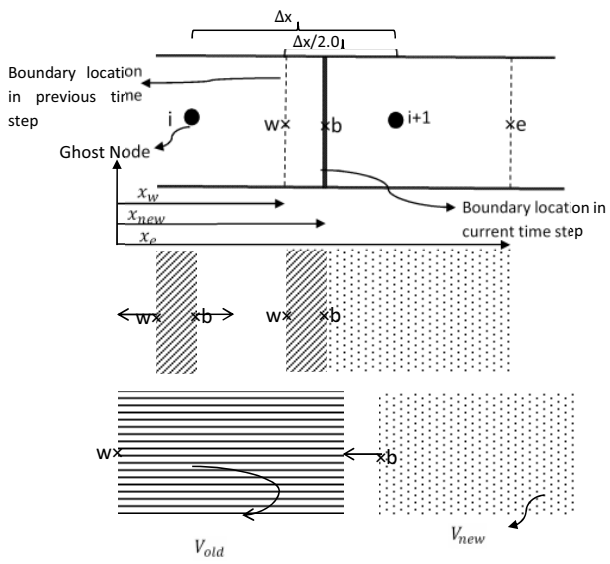

Fig. 5 Ghost Control Volume Type One

Now consider equations, (16) and (17) in a system of equations as follows.

$$\begin{cases} \rho\frac{(V_{old}-V_{new})-0}{\Delta t}+\rho(\hat{u}_b-\hat{u}_{cb})ds_x|_w \\ \quad +\rho(\hat{u}_b-\hat{u}_{cb})ds_x|_b=0 \\ \rho(\hat{u}_e-\hat{u}_{ce})ds_x|_e+\rho(\hat{u}_w-\hat{u}_{cw})ds_x|_w=0 \end{cases} \quad (18)$$

Solving this system of equations to eliminate mass flux on integration point w, one can get

$$-\rho\frac{(V_{old}-V_{new})-0}{\Delta t}+\rho(\hat{u}_b-\hat{u}_{cb})ds_x|_b + \rho(\hat{u}_e-\hat{u}_{ce})ds_x|_e=0 \quad (19)$$

and with a few simplifications get

$$\rho\frac{V_{new}-V_{old}}{\Delta t}+\rho(\hat{u}_b-\hat{u}_{cb})ds_x|_b+\rho(\hat{u}_e-\hat{u}_{ce})ds_x|_e=0 \quad (20)$$

Equation (21) is in fact the mass conservation equation for the real control volume between boundary b and the integration point e, as shown by dotted volume in Fig. 5. Therefore, with the above strategy boundary conditions can be handled merely by the ghost nodes and it does not need to cut boundary cells or control volumes. At the same time we have been able to implement conservation laws at the boundary control volumes.

We now explain the discretization of momentum conservation law for ghost control volume type two with the same procedure as discretization of mass conservation law. Mass conservation equation, (2), for the ghost control volume i, i.e. the volume with dashed diagonal lines in Fig. 5, is given bellow.

$$\rho\frac{(u_i^{new}(V_{old}-V_{new}))-u_i^{old}\times 0}{\Delta t} + \rho(\hat{u}_j-\hat{u}_{cj})uds_x|_b + \rho(\hat{u}_j-\hat{u}_{cj})uds_x|_w+Pds_x|_w^b=0 \quad (21)$$

In which the volume at the present time step is $V_{old}-V_{new}$, and the volume at the previous time step is zero. For the control volume of node i+1 (volume depicted with horizontal lines), momentum conservation equation can easily written as

$$\rho\frac{u_{i+1}^{new}V-u_{i+1}^{old}V}{\Delta t}+\rho(\hat{u}_e-\hat{u}_{ce})uds_x|_e+pds_x|_e + \rho(\hat{u}_w-\hat{u}_{cw})uds_x|_w+pds_x|_w=0 \quad (22)$$

Now consider equations, (21) and (22) in a system of equations as follows.

$$\begin{cases} \rho\dfrac{(u_i^{new}(V_{old}-V_{new}))-u_i^{old}\times 0}{\Delta t} \\ \quad +\rho(\hat{u}_w-\hat{u}_{cw})uds_x|_w \\ \quad +\rho(\hat{u}_b-\hat{u}_{cb})uds_x|_b+Pds_x|_b^w=0 \\ \rho\dfrac{u_{i+1}^{new}V-u_{i+1}^{old}V}{\Delta t}+\rho(\hat{u}_e-\hat{u}_{ce})uds_x|_e \\ +pds_x|_e+\rho(\hat{u}_w-\hat{u}_{cw})uds_x|_w+pds_x|_w=0 \end{cases} \quad (23)$$

Solving this system of equations to eliminate mass flux on integration point w, one can get

$$\rho\frac{u_{i+1}^{new}V-u_i^{new}V_{old}-u_{i+1}^{old}V+u_i^{new}V_{new}}{\Delta t} + \rho u(\hat{u}_e-\hat{u}_{ce})ds_x|_e+pds_x|_e+ \rho u(\hat{u}_b-\hat{u}_{cb})ds_x|_b+pds_x|_b=0 \quad (24)$$

and with a few simplifications such as $u_i = u_{i+1}$ we get

$$\rho\frac{u_{i+1}^{new}V_{new}-u_{i+1}^{old}V_{old}}{\Delta t}+\rho(\hat{u}_j-\hat{u}_{cj})uds_x|_e + \rho u(\hat{u}_b-\hat{u}_{cb})ds_x|_b+pds_x|_e + pds_x|_b=0 \quad (25)$$

Likewise what is described for discretization of mass equation, (25) is in fact the momentum conservation equation for the real control volume between boundary b and the integration point e, as shown by dotted volume in Fig. 5. This means that astrategy similar to mass conservation law can be applied for the momentum conservation law, i.e. there is no need to change the method of solution when boundary passes the integral point e.

The strategy implemented in this study is to remain in the IBM context. Therefore nodes within the flow field are always considered ordinary with complete control volumes. Boundary conditions are always implemented via the ghost nodes based on the conservation of conserved quantities. This is in contrast to other methods in which boundary conditions are applied using non-conserving methods such as linear, bilinear, and quadratic interpolations or extrapolations [21].

So far conserving methods such as cut cell [18], for a moving boundary problem, mass and momentum conservations laws are applied to the dotted area in Fig. 5 in ghost control volume type II, and to the dotted area in Fig. 4 plus the ordinary control volume of node i+1 in ghost control volume type I. As a result, in certain cases a larger than ordinary control volume is formed that may affect the accuracy of solution. However in the strategy proposed in this study, the control volume of node i+1 is always considered complete and unchanged, and for ghost nodes (type I and II), the conservation laws is applied to the area between the boundary and the integral point and this area never exceeds an ordinary control volume.

IV. Results

Present method is applied to a one dimensional, incompressible, inviscid moving boundary problem as shown in Fig. 6. A piston within a cylinder moves from its initial position to the right with a speed of $u_b$causing the fluid to flow out of the domain. Constant mass flow rate enters from the walls of the cylinder into the flow field. Ten control volumes are considered in this test case with an arrangement shown schematically in Fig. 7. According to the method presented in the previous section control volumes of node 3 to node 10, in this schematic, are considered as ordinary control volumes. Control volume of node 1 is out of calculation stencil, and control volume of node 2 would be a ghost control volume type one.

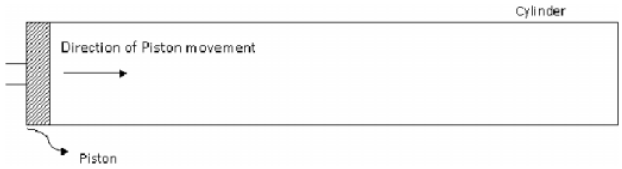

Fig. 6 Schematic of the test case studied here.

Cylinder length is assumed to be 1 meter, speed piston is constant and equal to 0.005m/s, and time step Δt is chosen to be 2 seconds. The back pressure is set equal to ambient pressure of 1 atm, and the constant mass flow rate of 0.01 kg/(m.s) is applied along the wall. Piston is initially positioned at node 1, and initial values ofzero velocity and atmospheric pressure are applied on the interior nodes.

Having solved this test case using the proposed method time variation of calculated piston pressure versus time is drawn in Fig. 8 with the thick solid line. In the first time step the piston pressure rises at once to slightly above the ambient pressure of 1 atm, and then decreases to ambient pressure in the following time steps which is according to the physics of the flow. Among sharp interface methods, the Image Point method of Ghias, et al., 2007, has been applied to this problem for comparison purpose.

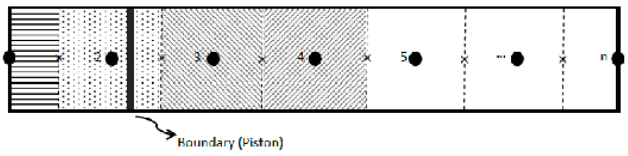

Fig. 7 Schematic of the control volumes of the test case studied here

Comparison between piston pressures calculated using this method and the method presented in this paper versus time are plotted in Fig. 8 As seen, oscillations occur in the results of Image Point method. This is in contrast to the results of the proposed method where no oscillations produced in the solution domain. This improvement in results is due to

conserving mass and momentum equations withoutany arbitrary boundary forcing or flow-field modification.

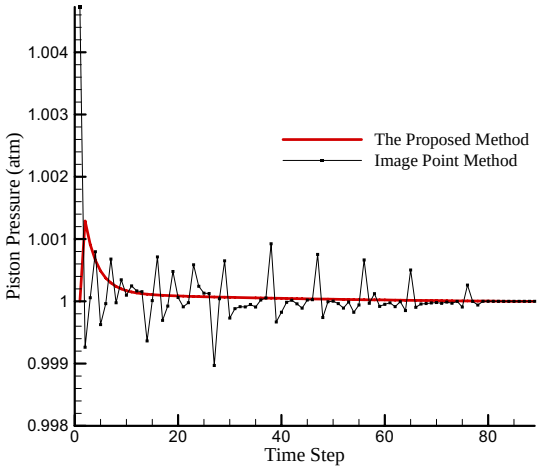

Fig. 8 Time variation of piston pressure along cylinder; comparison between the proposed method and the ordinary sharp interface method (Image Point)

Pressure distributions along the cylinder at different time steps calculated by the present method are plotted for different time steps in Fig. 9 Nodes numbers are tagged on the graph of2nd time step. Pressure decreases along the cylinder to ambient pressure at the end of the cylinder. While the piston moves down the cylinder the initial pressure also decreases. This decrease is consistent with a decrease of mass flow rate along cylinder during the piston movement. Note that as the piston moves toward the end of cylinder the surface through which the flow enters the cylinder decreases.

A graph similar to Fig. 9 is plotted using results of Image Point method in Fig. 11. In contrast to Fig. 10, pressure distribution along the cylinder does not obey a monotonic behaviour with time. As seen pressure distribution along the cylinder fluctuates with time.

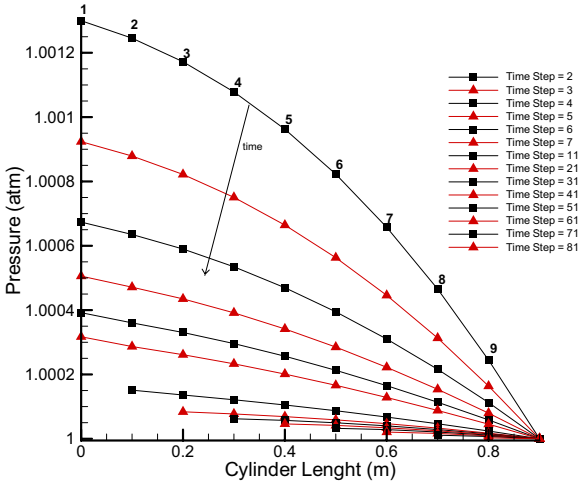

Fig. 9 Pressure distribution along the cylinder at different time steps calculated by the present method

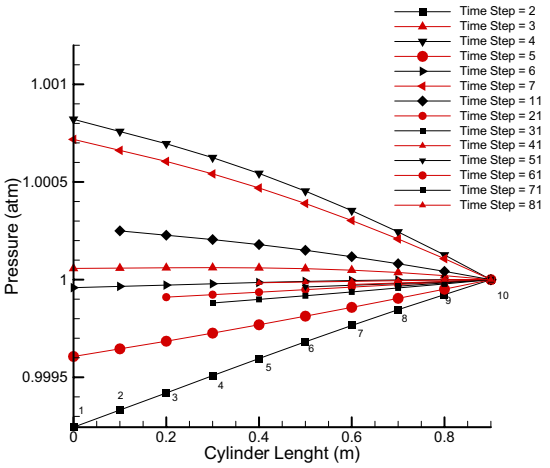

Fig. 10 Pressure distribution along the cylinder at different time steps calculated by the Image Point method

The velocities of the ghost and ordinary nodes along the cylinder versus their distance from the left end for different time steps obtained via our proposed method are plotted in Fig. 11. Each velocity diagram has an increasing rate along the cylinder length as the mass flow rate increases. The nodes velocity decreases in time as the piston moves toward the end of the cylinder while the amount of the mass entering the cylinder also decreases. The slopes in all the diagrams are the same and equal to the mass flow rate.

A similar diagram is presented in Fig. 12 based on the results of Image Point Method. In a quick look it can be seen that velocity diagram for time steps 12, 19 and 29 are quite similar to the results of our proposed method. After time step 29, velocities of ghost node experience a sharp increase compared to velocities of the following nodes, and the slope of velocity graphs has decreased for the following nodes, and also the velocity value for the final node is less than its actual value. These results show that our proposed method demonstrate a more accurate and consistent correspondence with the actual values in the velocity field.

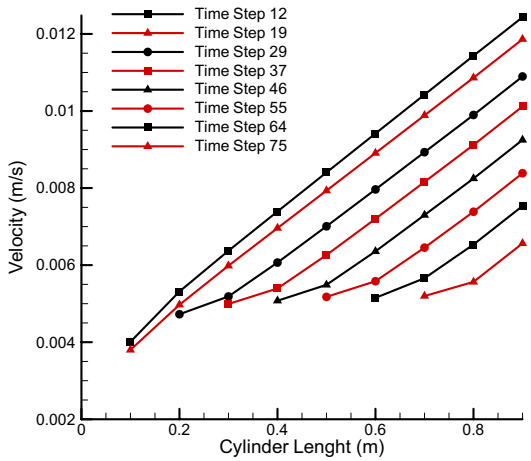

Fig. 11 Velocity of Nodes for several time steps via our proposed method

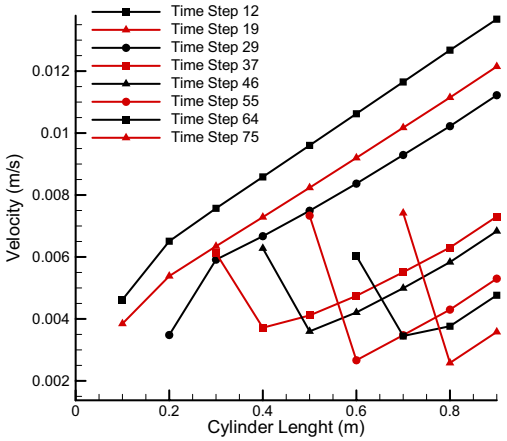

Fig. 12 Velocity of Nodes for several time steps via Image Point

The important criterion we believe that should be considered in comparison between two methods is the conservation of mass equation in ghost control volumes. Based on the following definition of mass conservation within the ghost nodes comparison between the two methods is depicted for this criterion in Fig. 13a, 13b and 13c.

It can be seen that mass equation is fully conserved via our proposed method (its deviation from mass equation is zero), while this is not the case in the Image Point method and deviation from full conservation is seen for this method. Similar to previous diagrams the higher the mass flow rate, the larger is the deviation from conservation of mass.

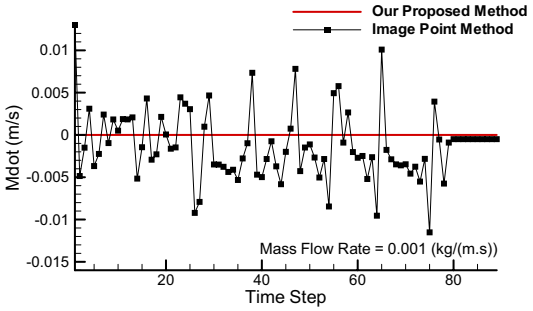

Fig. 13a Deviation from mass conservation equation by the two methods (mass flow rate 0.0005 (kg/(m.s))

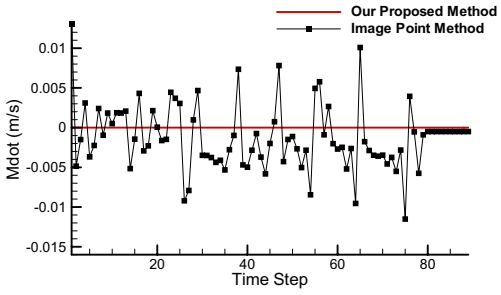

Fig. 13b Deviation from mass conservation equation by the two methods (mass flow rate 0.001 (kg/(m.s))

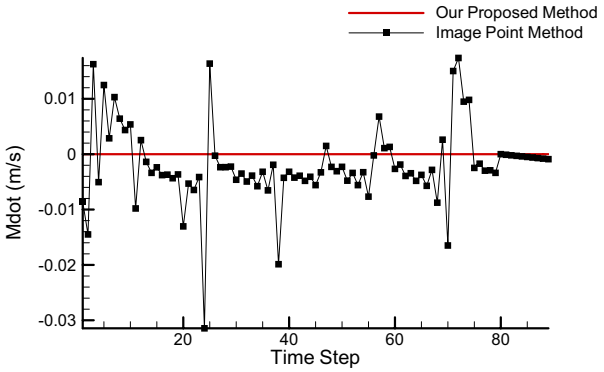

Fig. 13c Deviation from mass conservation equation by the two methods (mass flow rate 0.002 (kg/(m.s))

V. Conclusions

AnIBM-based new algorithm applying boundary conditions by fully conserving mass and momentum equations is presented to solve flow field. The algorithm is applied to a one-dimensional, incompressible, inviscid flow including mass source in a moving boundary problem and compared to a sharp interface i.e. Image Point method. Modeling this case by Image point method showed some spurious pressure oscillation, while pressure fluctuations are fully resolved using the method proposed in the current study. Moreover, the Image Point model shows a discontinuity in the velocity field between the piston and the following nodes (i.e. nodes coming after the first one) velocities. Also as time passes, the velocity values become less than their actual ones. In the method proposed in this study, no discontinuity appears in the velocity field and also the nodes velocity values are more accurate.

It is concluded that the current proposed algorithm is not problem based and simulate flow field by solving mass and momentum equations completely, without any assumption or simplification. While in simpler cases, especially non-moving problems, where pressure and velocity fields are consistent with their type and degree, sharp interface methods are simpler modeling choices, in generally moving boundary problems with and without source of mass, the new proposed algorithm introduced in this study presents more reliable results.

References

[1] PESKIN, C. S. Flow patterns around heart valves: A numerical method. Computational Physics, v. 10, p. 252-71, 1972.PESKIN, C. S. The fluid dynamics of heart valves: experimental, theoretical and computational methods. Annual Review. Fluid Mechanic, v. 14, p. 235–59, 1981.

[2] BERGER, M.; AFTOSMIS, M. Aspects (and aspect ratios) of cartesian mesh methods. [S.l.]: Proc. 16th Int. Conf. Numerical Methods Fluid. 1998.

[3] LAI, M.; PESKIN, C. An immersed boundary method with formal second-order accuracy and reduced numerical viscosity. Computational Physics, v. 160, p. 705–19, 2000.

[4] SAIKI, E.; BIRINGEN, S. Numerical simulation of a cylinder in uniform flow: application of a virtual boundary method, v. 123, p. 450–65, 1996.

[5] GOLDSTEIN, D.; HANDLER, R.; SIROVICH, L. Modeling a no-slip flow boundary with an external force field. Computational Physics, v. 105, p. 354–66, 1993.

[6] IACCARINO, G.; VERZICCO, R. Immersed boundary technique for turbulent flow simulations. Mechanical Review, v. 56, p. 331–47, 2003.
[7] ANGOT, P.; BRUNEAU, C.; FRABRIE, P. Apenalization method to take into account obstacles in viscous flows. Numerical Mathematics, v. 81, p. 497–520, 1999.
[8] KHADRA, K. et al. Fictitious domain approach for numerical modeling of Navier-Stokes equations. Numerical Methods Fluids, v. 34, p. 651-84, 2000.
[9] MAJUMDAR, S.; IACCARINO, G.; DURBIN, P. RANS solver with adaptive structured boundary non-conforming grids. Cent. Turbul. Res. , n. 2001, , p. 353–64, 2001.
[10] GHIAS, R.; MITTAL, R.; LUND, T. A non-body conformal grid method for simulation of compressible flows with complex immersed boundaries. AIAA, p. 2004-0080, 2004.
[11] GHIAS, R.; MITTAL, R.; DONG, H. A sharp interface immersed boundary method for compressible viscous flows. computational phusics, v. 225, p. 528-53, 2007.
[12] CLARKE, D.; M., S.; H., H. Euler calculations for multi-element airfoils using Cartesian grids. AIAA, v. 24, p. 1128–35, 1986.
[13] ZEEUW, D.; POWELL, K. An adaptively refined cartesian mesh solver for the Euler equations. AIAA, v. 1991-1542, 1991.
[14] UDAYKUMAR, H.; SHYY, W.; RAO, M. Elafint: A mixed Eulerian-Lagrangian method for fluid flows with complex and moving boundaries. Numerical Methods, v. 22, p. 691–705, 1996.
[15] UDAYKUMAR, H. et al. A sharp interface cartesian grid method for simulating flows with complex moving boundaries. Computational physics, v. 174, p. 345–80, 2001.
[16] UDAYKUMAR, H.; MITTAL, R.; RAMPUNGGOON. Interface tracking finite volume method for complex solid-fluid interactions on fixed meshes. Commun. Numerical Methods Engineering, v. 18, p. 89–97, 2002.
[17] YE, T. et al. An accurate cartesian grid method for viscous incompressible flows with complex immersed boundaries. Computational Physics, v. 156, p. 209–40, 1999.
[18] KARIMIAN, S. M. H.; AMOLI, A.; MAZAHERI, K. Control-volume finite-element method for the solution of 2D euler equations on unstructured moving grids. Iranian Journal of Science & Technology, v. 26, p. 465-76 , 2002.
[19] KARIMIAN, S. M. H.; SCHNEIDER, G. E. Pressure-Based computational method for compressible and incompressible flows. AIAA, Journal of Thermodynamics and heat transfer, v. 8, p. 267-74, 1994.
[20] MITTAL, R.; IACCARINO, G. Immersed Boundary Methods. Fluid Mechanics, v. 37, p. 239-61, 2005.